Design of Composite Floors with Profiled Steel Sheet

Jan W. B. Stark

DESIGN OF COMPOSITE FLOORS WITH PROFILED STEEL SHEET

by Jan Stark*

1. INTRODUCTION

Besides the many types of floors of reinforced concrete (mainly prefabricated) and brick materials that are used in the Netherlands, there is now a growing interest in floors composed of thin, profiled, steel sheets combined with concrete. Profiled steel sheet can be applied for floor slabs in three different ways:

a) Steel sheet as formwork

Here the profiled steel sheet serves only as permanent formwork for the concrete. The floor slab has to be reinforced in the normal manner.

b) Steel sheet as deck

The steel sheet is the only structural element. The concrete serves for load distribution and surface element. Cellular sections may be used for installation purposes.

c) Steel sheet as formwork and reinforcement

In the above two forms of construction the steel and concrete are not both fully utilised. In this aspect a better form of construction is obtained when the steel sheet is connected to the concrete to resist the shear forces between the two materials. In this way a composite element is obtained comparable with a steel-concrete composite beam. The steel sheet has a dual function as a permanent formwork and as positive reinforcement of the slab.

---

* Head of the Department of Steel Structures, Institute TNO for Building Materials and Building Structures, Delft, the Netherlands.

The common name for this type is: composite floor.

In Holland applications type a) and b) are in general not competitive. Type c) the composite floor, may be competitive when besides the price per m^2, the following advantages are taken into account:

- Because of the dual function of the steel sheet time is saved, since no extra reinforcement has to be layed; the form is simple and needs few supports; striking and cleaning of the formwork for re-use is not necessary.
- Erection time is quicker since the sheets arrive on site ready to be placed.
- The steel sheets provide a working platform for casting the concrete and provide protection to the lower floors.
- During erection the lateral instability of the main beams is prevented by the sheets.
- Most products have standard fixtures for ceilings and installations. Cellular steel sheets can be used. This enables the lay-out of installations for offices etc. to be much more flexible.

Therefore in this paper only floors of type c) will be discussed. From the definition appears clearly that it is essential that the steel sheet is adequately connected to the concrete. This connection can be achieved in three different ways, each with specific mechanical properties.

Type 1: Effective bond ensured by the profile shape

The connection between the steel sheet and the concrete is achieved by surface bond. The steel sheet should have dovetailed troughs or another shape with re-entrant corners. Due to the interlocking shape separation is prevented and a reliable effective bond can develop.

Examples of this type, used in Holland, are Holorib (Fig. 1) and Lewis. The Holorib sheet is available in two depths namely 38 mm and 51 mm and various thicknesses. The Lewis sheet has rather small dimensions (depth 15 mm, thickness 0.5 mm) and is intended to be used for concrete floors of small size on timber beams (f.c. in renovation).

Type 2: Indentations in the profiled sheet

The shear resistance between the steel and the concrete is improved by rolling into the flanges and/or the webs of the sheeting some kind of indentations. Examples of this type used in Holland are Cofrastra, Prins floor, Hi-Bond and Robertson Q-lock (see Fig. 2). The depth of the sheets ranges from 40 mm up to 77 mm and sheet thickness from 0.75 mm up to 1.25 mm. When the sheet is trapezoidal profiled the indentations must also be able to prevent separation. Composite action is dependent on the type of sheet, depth and number of indentations and the span of the slab. Tolerances in form and depth of the indentations may have a considerable influence on the shear capacity.

Type 3: Additional anchors

Anchors may be provided to produce composite action with plain profiled sheets or to enhance the load-carrying capacity when indented sheets are used.
An example of anchors positioned throughout the span are reinforcement bars welded over the troughs of a sheet (Fig. 4). This type is not used frequently in Holland because fabrication costs are too high.
Another possibility is to provide anchorages at the ends of each span preventing slip between the concrete and the sheet. The anchorages may take the form illustrated in Figure 5.
At this moment only the headed stud can lead to an economic solution. The connector can then be used in triple function namely:

- fastening of the sheet ('weld-trough', Fig. 6);
- end anchorage for the slab;
- shear connector to achieve composite action of composite slab with supporting beams.

2. PROPERTIES OF A COMPOSITE SLAB IN BENDING

2.1 Principal failure modes

Composite slabs are essentially made from simular component parts as a composite beam namely a steel section (profiled sheet) and a concrete slab which are connected to resist longitudinal shear forces. It is therefore logical to assume that a composite slab will have simular properties as a composite beam.
For a simply-supported slab the ultimate load can be determined by three principal criteria. Or in other words, a slab can fail in three different ways. Figure 8 shows the sections which are characteristic for these criteria.

Section I: Vertical shear capacity of the slab

This criterium normally will not be critical because composite slabs are relatively slender elements. It may be critical in special cases e.g. deep slabs of short span with relatively high loads.

Section II: Moment capacity

In this case the slab will fail in a flexural failure mode. The maximum load is reached when in the critical section the optimum stress situation is reached. In Figure 9 this stress situation is shown for a so called 'low-reinforced' slab, where the full steel section can yield in tension ($\epsilon \geq \epsilon_y$) before the crushing strain of concrete in the upper fiber is attained. From equilibrium condition follows that this optimum stress situation can only be reached if in section III-III a longitudinal shear force S_{max} can be transmitted that is at least equal to the resulting tensile force in the steel ($T = A\sigma_e$). This is defined as a complete shear connection.

Section III: Longitudinal shear capacity

In this case the slab will fail in a longitudinal shear failure mode.

The maximum moment depends on the degree of connection present at the interface between the concrete and the steel or in other words depends on the magnitude of the longitudinal shear force S_{max} at failure. The optimum stress situation and so the ultimate moment in section II can not be reached. This is defined as incomplete shear connection.

2.2. Slabs with complete shear connection

If there is complete interaction - that means no slip between the steel sheet and the concrete - it may be assumed that plane sections remain plane after bending. If the stress-strain relations of the two materials are known, it is possible to find the stress distribution for every value of the curvature. From the stress distribution follows the moment and so the relation between moment and curvature can be determined.

For mild steel a good and safe approximation of the real σ-ε-relation is given by the ideal elastic-plastic diagram shown in Figure 10a.

The stress-strain relation of concrete is not only influenced by the quality of the concrete but also by the speed of loading and the form and dimensions of the test specimen. Figure 11 shows for example the influence of loading speed on the stress-strain relation found with an uniaxial compression test on a prism. For design purposes these σ-ε-relations are not very suitable. Therefore the CEB has agreed upon an idealisation of this relation as shown in Figure 10b. Because the falling branch is not included, it was necessary to limit the maximum compressive strain: $\varepsilon_u' = 3.5^{o}/oo$. When the idealised σ-ε-diagrams of Figure 10 are used, the theoretical ultimate moment is reached when in the outer fiber of the concrete, the strain is equal to ε_u'.

Depending on the position of the neutral axis different stress situations at ultimate moment are possible as shown in Figure 12. Only for case (a), when the steel sheet is fully plastified a simple design formula can be derived. For the other cases the calculation of the ultimate moment is more complicated. For design purposes therefore, a simplified method is generally adopted.

The basic assumption for this design method is that both steel and concrete are assumed to be ideal plastic materials. For steel this is a usual assumption for example also adopted in plastic design of steel structures.

For concrete the difference between the real and the idealised stress-strain relation is greater. To compensate the effect of this unsafe idealisation, the ultimate stress of the concrete is reduced with a factor k. Calculations for a great number of composite sections have shown that a safe estimation of the ultimate moment can be found if the value of k is assumed to be 0.8.

The idealised stress-strain diagrams are drawn in Figure 13. Using these ideal plastic stress-strain relations means that the ultimate moment of the section only follows from equilibrium conditions. There are two possible cases to be considered, depending on the position of the neutral axis at ultimate load as shown in Figure 14.

The fact that the ultimate moment M_u can be determined from equilibrium conditions means that M_u is not influenced by internal forces caused by the manufacturing process. So a composite slab not propped during casting of the concrete will have the same ultimate load as when propped.

This may be illustrated by the results of load tests on two simply supported Prins-floors with a total depth of 120 mm and a span of 3.80 m. One was propped during casting of the concrete, the other one unpropped. In Figure 15 the measured relationship between load and deflection is given. The non-supported slab II, with initial steel stresses due to casting equal to σ_a = 115 N/mm^2, appeared to be even stronger than the propped slab I.

2.3. Slabs with incomplete shear connection

Imcomplete shear connection implies that a horizontal shear failure occurs before the optimum stress situation as shown in Figure 9 is attained. The failure load can be calculated when the stress situation and so the moment in the heaviest loaded section is known. This stress situation is of course dependent of the strength of the shear connection. However, this is not the only parameter because the deformation capacity of the shear connection also plays an important role. This is illustrated in Figure 16 where as an example the stress situation is presented for two extreme cases e.g. an extreme brittle shear connection (bond) and an ideal tough shear connection.

In the case of a brittle shear connection the maximum moment is reached when shear failure starts. Because of the sudden drop-of of the shear load when slip occurs also the moment and the load show a sudden decrease. Until the maximum load is reached, plane sections remain plane (no slip). From this compatibility condition and equilibrium between shear force S_{max} and tensile force T follows the stress situation.

When the shear connection is tough no drop-of of load occurs when S_{max} is reached. When slip increases the magnitude of S_{max} remains constant. As a result of the slip the curvature increases with constant value of T and D (see Fig.16). Because of that, the steel and the concrete have no longer a common neutral axis. A redistribution of stresses is possible so that an optimum situation can be attained. The stress situation then only follows from the yield condition and the equilibrium between T and S_{max}. The influence of the deformation capacity appears clearly from Figure 17, where for a specific slab the relation between moment and shear load is shown for the two extreme cases of deformation capacity and with same shear strength.

When infinite rotation capacity of the shear connection is assumed the relation between maximum moment and the ultimate shear strength S_{max} can simply be calculated. A qualitive presentation of this relation is given in Figure 18. Now it has been shown that the deformation capacity of the shear connection is an important parameter, it will not be surprising that the properties of slabs with plain sheets are quite different from those with some kind of mechanical shear connection. This is illustrated more in detail in section 3 and 4 where some theoretical consideration and test results for a specific product of both types will be presented.

3. DESIGN OF COMPOSITE SLABS WITH PLANE SHEETS

When the concrete in tension is uncracked ($M_{max} < M_{crack}$) the shear stress at the interface between concrete and steel can be calculated with the well-known formula:

$$\tau = \frac{VQ}{bI_c} \qquad \text{-------} \qquad (1)$$

where: V = shear force

Q = statical moment of concrete sectional area

b = width

I_c = composite section moment of inertia

The value of the shear stress is maximum near the support.
Some manufacturers of composite decks used this formula to check for the horizontal shear criterium. Based on tests a limiting value for the shear stress τ was determined (see for example [1]).
It will be shown now that this design method must be used with care and only applies if the slab dimensions and the load pattern are approximately the same

as in the tests.

Assuming that the formula (1) applies the total ultimate load (= 2V) should only be dependent of the cross-sectional dimensions of the slab and should be independent of the loading scheme and the span. Slip should start near the supports where the shear force and thus the shear stress is maximum. In the table of Figure 19 results are presented of load tests on simply-supported Holorib-slabs, type 38/0.91, 120 mm deep, 0.47 m wide and spanning 4.0 m.

The slabs were continuously supported during casting and hardening of the concrete. From the table appears that the shear force at failure was not the same for all the tests with a shear failure mode.Furthermore during the test was visually found that slip did not start near the support but at the section of maximum moment. This behaviour can be explained as follows. From the measured load-deflection curves can be determined that the cracking moment was approximately 6 kNm. Before that value is reached the horizontal shear stress is still very small. When cracking occurs, the stress in the steel at the position of the crack will be considerably higher than at the uncracked sections surrounding the crack; thus the local shear stress between the steel and the concrete increases considerably (see Fig. 20). If the critical value of the bond stress is reached, slip between concrete and steel will start. This means that friction forces will develop with the result that at sections further from the crack a smaller shear force has to be transmitted. With increasing loading, also in these sections the critical bond stress will be attained. Loss of bond will proceed over a continuously increasing length. The slab more and more acts as a 'tied arch' as illustrated in Figure 21. As soon as the anchorage length of the tie is too short, the slab will fail.

The facts seem to confirm this theory:

- Test specimen 7 (table fig. 19) has a considerable higher ultimate moment then the other specimens. Failing of the anchorage of the tie is prevented by the shear connectors.

- The ultimate moment is higher when the distance of the relevant section to the support is greater.

In [2] Bryl reaches the same conclusion and proposed as a safe criterion for failure the moment when cracking occurs in the concrete. This appears to be an overconservative approach.

In Figure 22 the ultimate moment from the tests recorded in Figure 19 have been plotted against the shear span, ℓ_s. It appears that the ultimate moment increases proportionately with the shear span. This is a logical result, since, if the slab is very long shear failure will not occur but flexural failure ($M_{max} = M_u$).

For design purposes the relation as presented in Figure 22 can be derived for various floor types by performance tests. This method of presentation has the advantage showing very clearly the efficiency of the relevant system.

4. DESIGN OF COMPOSITE SLABS WITH DEEP INDENTED SHEETS

In this section will be shown that the theory presented in 2.3 for slabs with incomplete shear connection with 'tough' connectors, can be applied for indented sheets provided the indentations are deep enough.

For the Dutch product "Prins-floor" an extensive test programme has been carried out to confirm this. The Prins sheet is a trapezoidal profiled sheet. In the webs are rolled two rows of spherical indentations (burls). The horizontal spacing of the indentations is 30 mm and the depth is 4 mm.

Figure 23 gives an impression of the sheet. When it is assumed that the burls behave 'tough', the ultimate moment can be calculated if the ultimate shear force per burl is known.

According to the theory presented in section 2.3 in the region of the maximum moment a fully plastic stress distribution is assumed. The compressive force in the concrete (= tensile force in the steel sheet) equals the resultant ultimate shear force of the burls (= n S_u) over the shear span. The ultimate moment can be calculated from the so found stress distribution (see Fig. 24).

To simplify the calculation, the stress distritution in the sheet can be split in two components; pure tensile force resp. pure bending moment.

The ultimate shear force per burl is determined from beam tests with variable spans and floor depths. The tests loads were 4 line loads as shown in Figure 25. Figure 26 shows the measured relation between load and deflection resp. load and end slip for an element with 5.0 m span and a depth of 160 mm. These two plots show clearly the ductile behaviour of the burls. After the slip starts the load can still be increased and when the ultimate load is reached with increasing slip load remains practically constant (horizontal branch).

Figure 27 gives an impression of a test specimen after the test. From the tests followed that, when the length of the shear span is so long, that it contains about 210 burls per web, the optimum stress distribution can be reached. The tested slabs had 6 webs over the width. The yield force of the steel sheet was $A\ \sigma_y$ = 297 kN.

So the ultimate shear force per burl can be calculated as:

$$S_u = \frac{A\ \sigma_y}{n} = \frac{297000}{6 \times 210} = 238 \text{ N}$$

With the theory, discussed before, the relationship is determined between the maximum moment and the number of burls in the shear span (or here equivalent the length of the shear span). The calculated relation is plotted in the graph of Figure 28, together with some test results. With the burl configuration of the normal Prins product, within practical values of the span, the ultimate capacity of the shear connection will be not less then 0.7 A σ_y. However in a preliminary test programme sheets have been tested with larger burl spacing. Some of the results of these preliminary tests are plotted as well in Figure 28 (solid dots). The comparison is not fully justified, because the sheets for the preliminary tests were fabricated in a different way then the final product. As a results of that the shape of the burls was slightly different. As mentioned before the shape of the indentations has a considerable influence on the ultimate shear capacity. Worth mentioning as well is that the ultimate load was unfavourably influenced because the outer webs of the sheets were not lateral supported. The webs deformed as shown in Figure 29, and caused the burls in these webs to be less effective. In a real structure this deformation cannot occur because the adjacent slabs give the necessary support. The test results are therefore conservative. To obtain more information about the influence of the concrete quality on the maximum load per burl, also push-out tests have been carried out after the bending tests. The principle is shown in Figure 30. Contrary to the bending test now the outer webs were lateral supported.

With a cube strength of 36 N/mm^2 (same as in bending tests) the ultimate shear load per burl was 287 N. The difference of 15% between the result of the bending tests and the push-out tests can be fully ascribed to the influence of the edge condition of the outer webs.

It can be concluded that for the investigated type the design method for tough connection as presented in section 2.3 may be applied. With this method design tables have been produced by the manufacturer [3].

5. RESEARCH ACTIVITIES IN EUROPE

At this moment a number of research institutes in different countries in Europe are involved with research on composite decks.
Without being complete the following institutes can be mentioned:

England : University of Salford, Department of Civil Engineering, Prof. E.R. Bryan and Mr D.C. O'Leary.

France : Centre Technique Industriel de la Construction Métallique, Mr A. Fulop and Mr C. Moum.

Germany : .Institut für Konstruktiven Ingenieurbau, Ruhr Universität Bochum, Prof. K. Roik and Dr B. Hofmann (now Hoesch Siegerlandwerke AG).
.Institut für Statik und Stahlbau der Technische Hochschule Darmstadt, Prof.dr ing. O. Jungbluth and Mr R. Gräfe.

Netherlands : Institute TNO for Building Materials and Building Structures, Ir J.W.B. Stark.

Switserland : Institut für Stahlbau der Eidgen. Technische Hochschule Lausanne, Prof.dr J.C. Badoux and Mr M. Crisinel.

Some publications are mentioned in the reference list |1|, |4|, |5|, |6|.

In 1975 the European Convention for Constructional Steelwork (ECCS) presented European recommendations for the design of composite floors with profiled sheet |7|. The draft of these recommendations was prepared by the Department of Civil Engineering of the University of Salford. A working group of committee 11 of the ECCS, under chairmanschip of Prof. F. Reinitzhuber, was entrusted with the elaboration of the recommendations.
The recommendations were based on the state of the art at that moment.
Recently new design methods for composite floors have been developed. So a

revision of the recommendations are under preparation. This revision will be prepared by a working group of Commission Mixtes (AIPC-CEB-CECM-FIP) and will form part of European recommendations for all types of composite construction.

APPENDIX 1 - REFERENCES

|1| Prof.Dr J.C. Badoux, M. Crisinel, "Recommendations par l'utilisation de toles profilees dans les planchers mixtes du batiment", Schweizerische Zentralstelle für Stahlbau, Zürich, 1973.

|2| S. Bryl, "Die Verbundwirkung zwischen profiliertem Stahlblech und Beton in Deckenplatten", Acier, Stahl, Steel, 1967 no 10.

|3| Prins N.V.,"The design of Prins composite floors, type PSV-73", Dokkum, 1972.

|4| A. Fulop, C. Moum, "Rapport General sur l'interpretation des essais en flexion des planchers mixtes a bacs collaborants", CTICM-report, April 1976.

|5| B. Hofmann, "Decken und Trägerverbund bei Verwendung von Stahlprofilblech - Verbunddecken", Ruhr Universität Bochum, 1975.

|6| R. Gräfe, "Verdübelung und Tragverhalten von Stahlprofielblech/Beton - Verbundplatten", Dissertation Technische Hochschule Darmstadt, 1976.

|7| ECCS (published by Constrado), "European Recommendations for the design of composite floors with profiled steel sheet", London, May 1975.

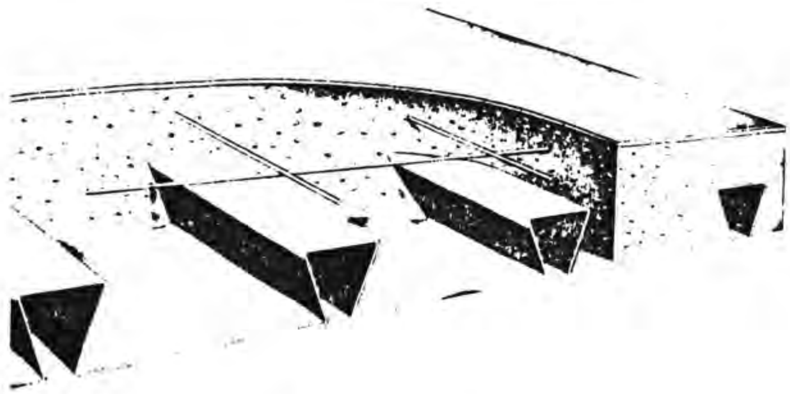

Fig.1 Composite floor – Holorib system

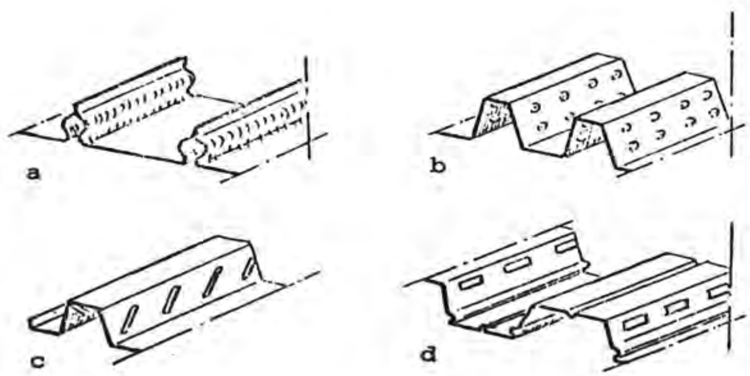

a. Shaped troughs with small deformations
b Spherical dents in the webs
c Inclined lugs in the webs
d Cusps on the webs and longitudinal dimples

Fig.2 Some types of sheets with indentations.

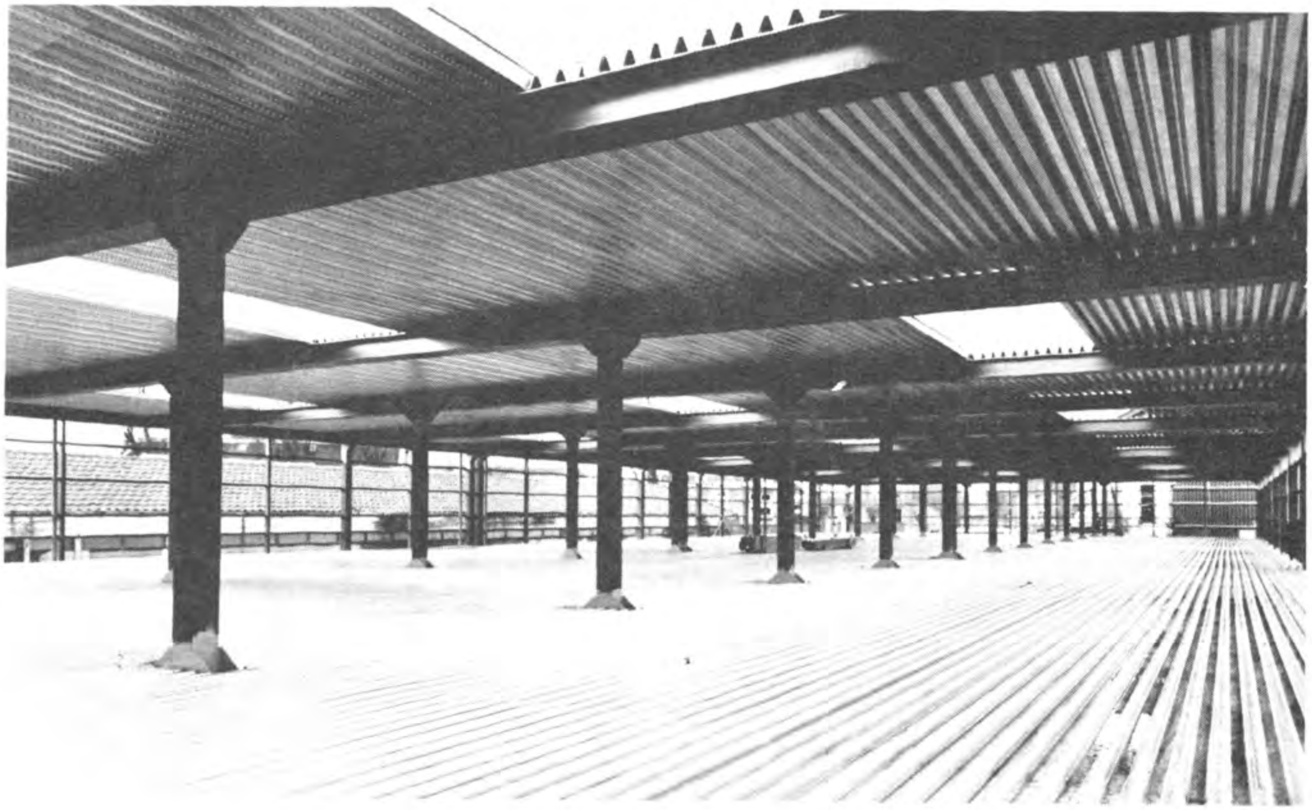

Fig. 3 Prins system, steel sheet with indentations.

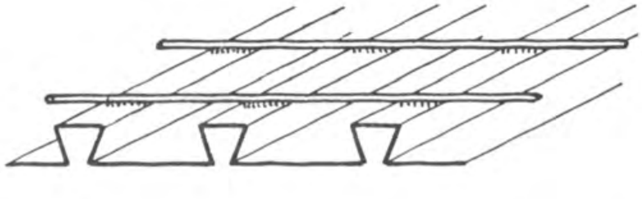

Fig. 4 Reinforcement bars welded over the troughs as additional anchorage.

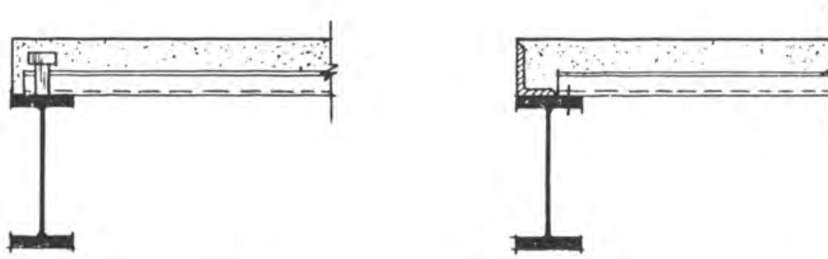

Fig. 5 Anchorage at end support.

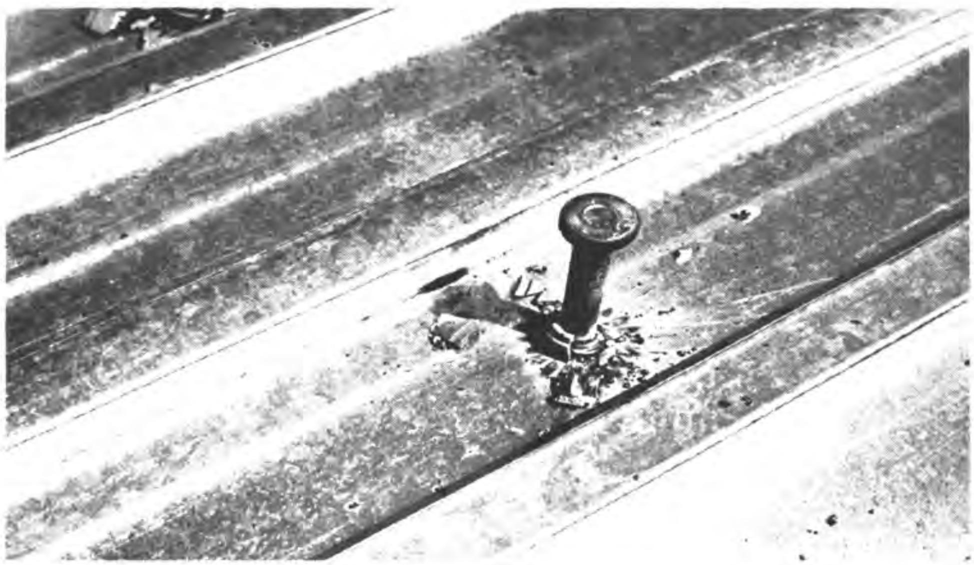

Fig. 6 Headed stud welded through the steel sheet.

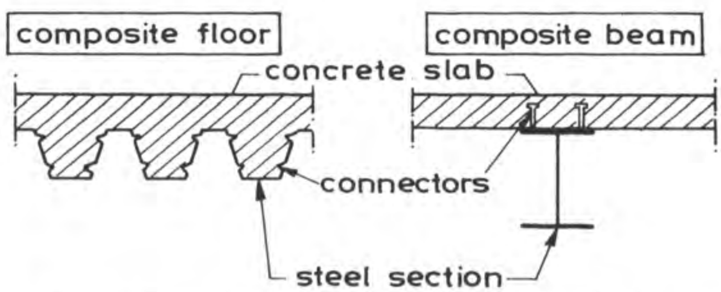

Comparison of a composite floor with a composite beam.

Fig. 7

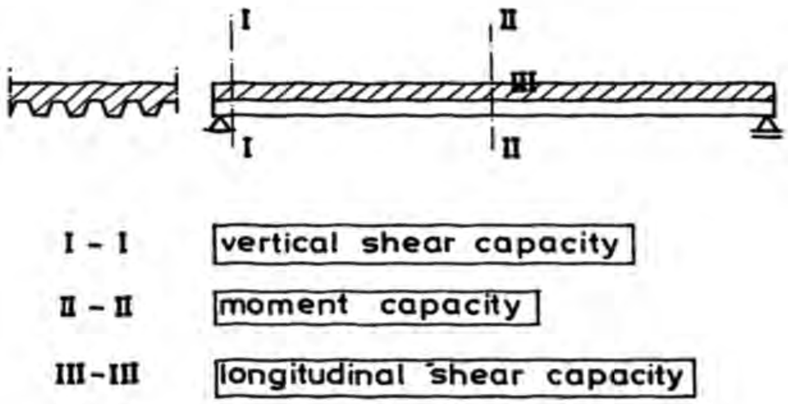

Sections which may be critical

Fig.8

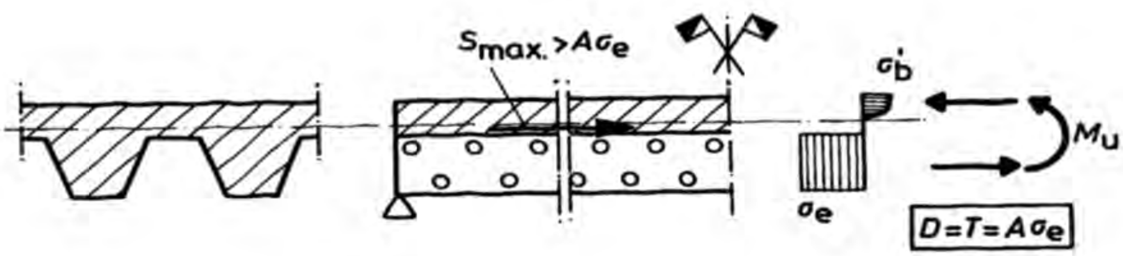

Optimum stress situation in a "low-reinforced" composite floor.

Fig. 9

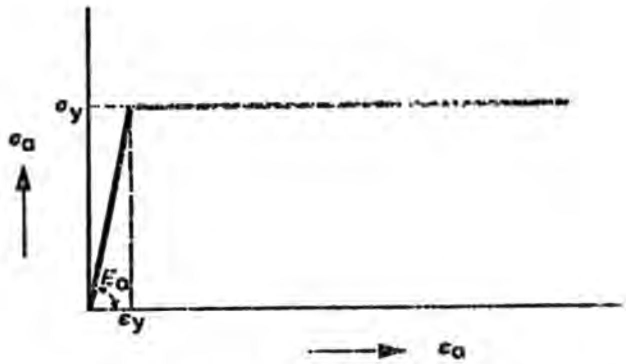

a. Ideal elastic-plastic stress-strain diagram.

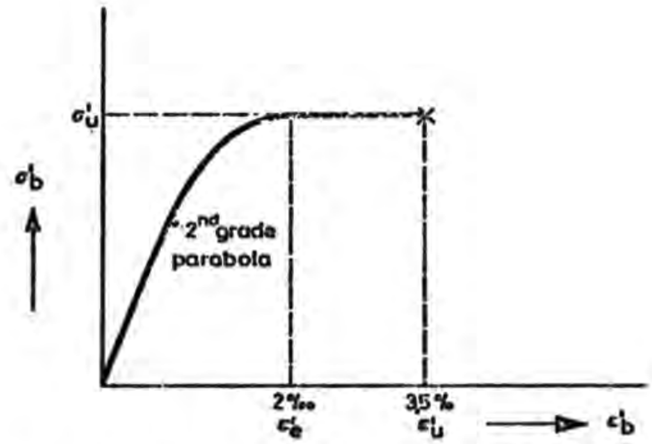

b. Idealized $\sigma-\varepsilon$ diagram of concrete for short time loading. (CEB)

Fig. 10

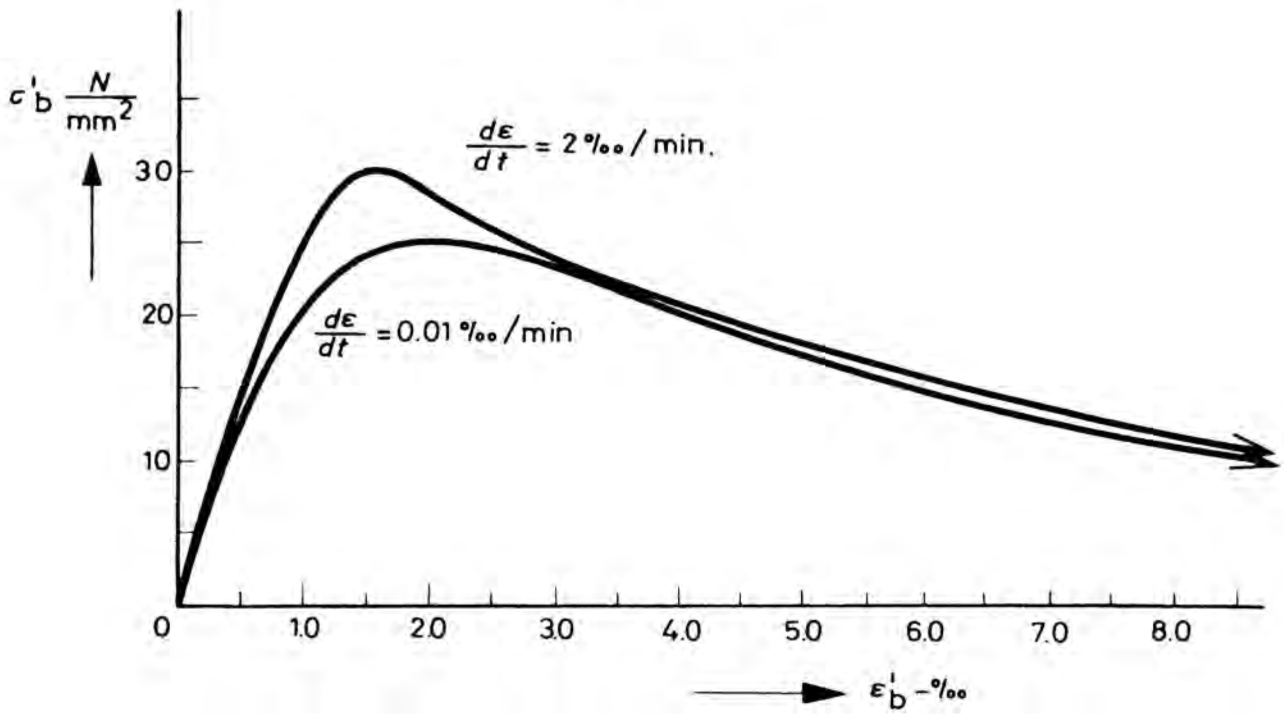

Stress-strain relations for concrete (compression test on prism).

Fig. 11

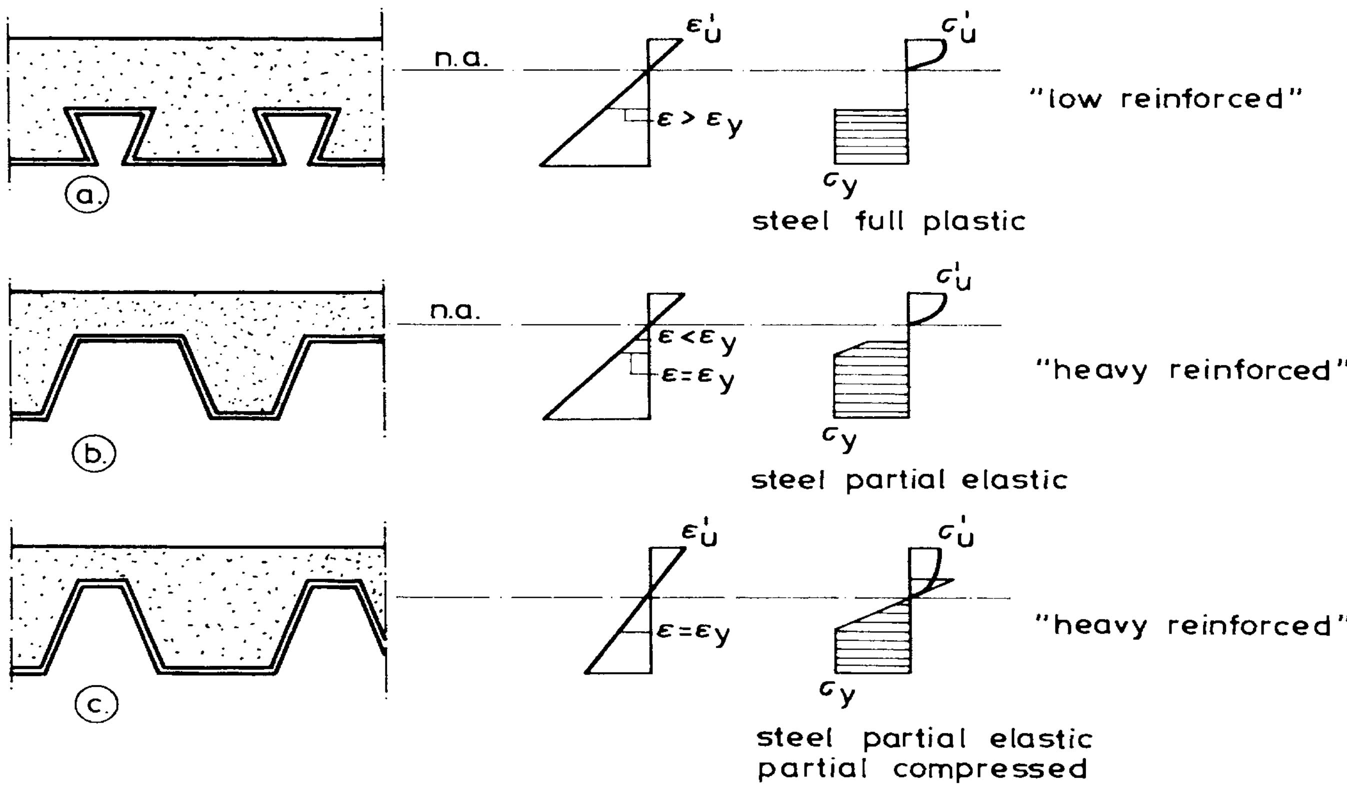

Different possible stress situations

Fig.12

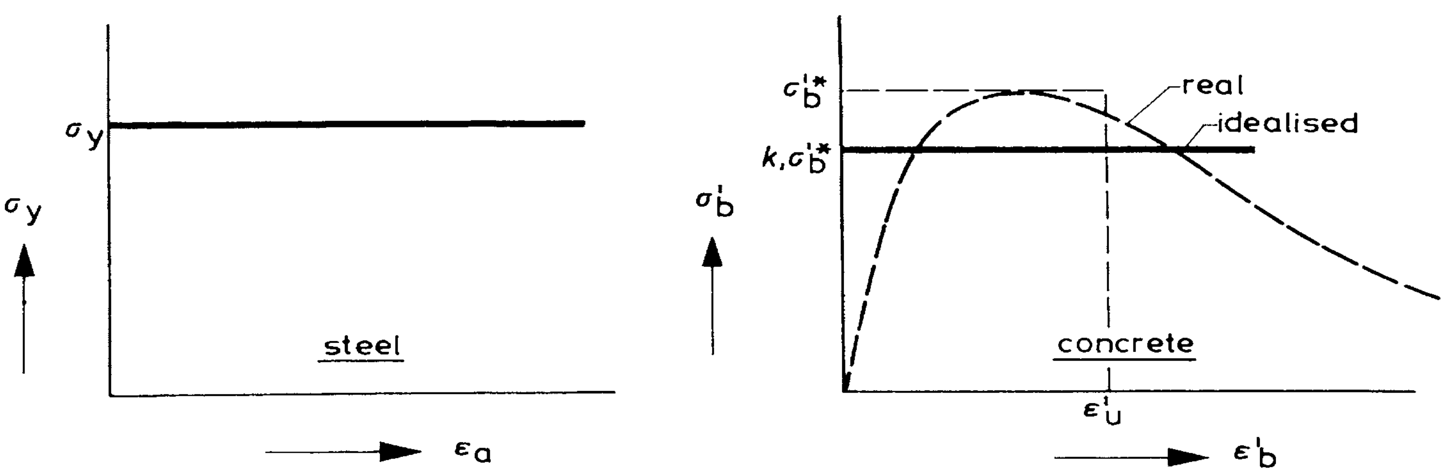

Idealised "ideal plastic" $\sigma - \varepsilon$ diagrams

Fig.13

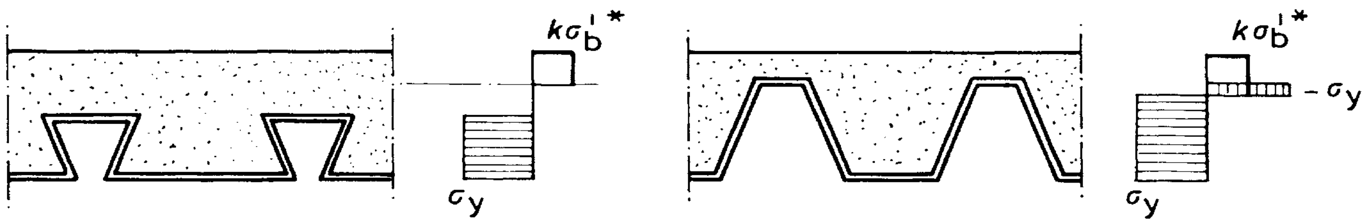

Possible stress distribution at ultimate load using "ideal plastic" $\sigma - \varepsilon$ relations.

Fig.14

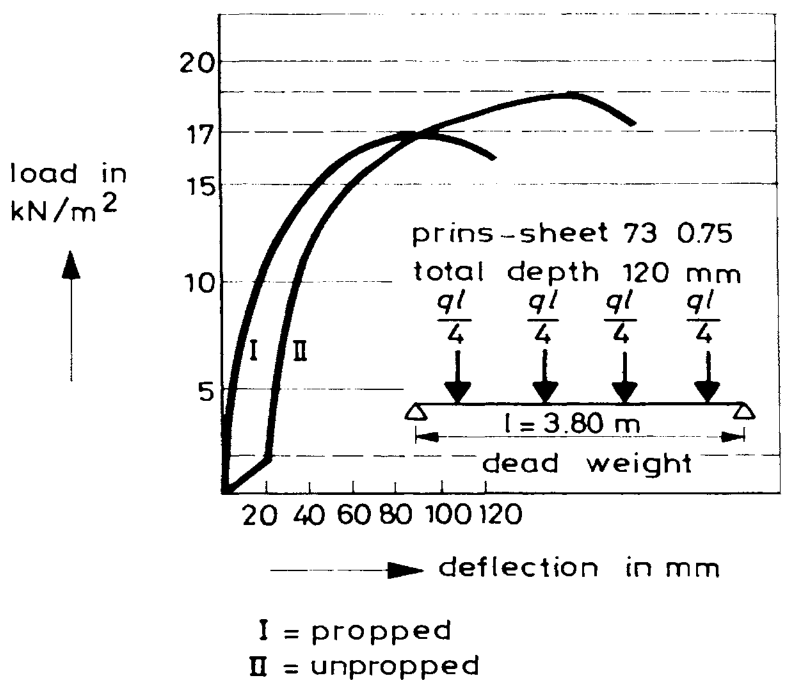

Measured load-deflection diagrams

Fig. 15

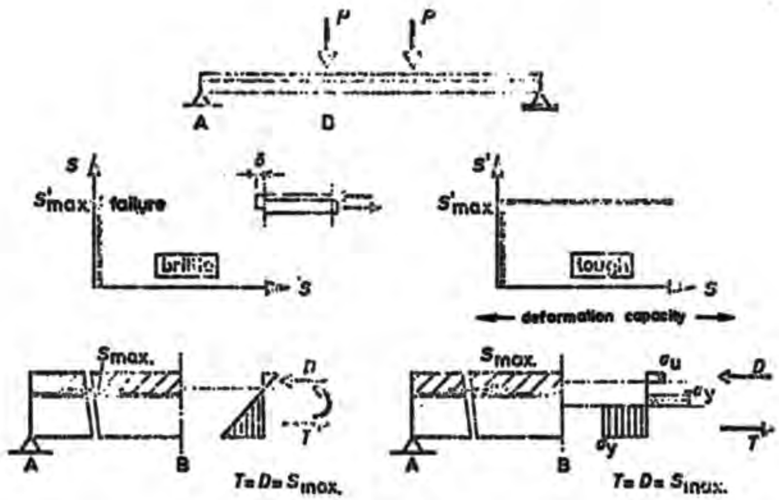

Stress situation at shear failure for a brittle resp. a tough shear connection.

Fig.16

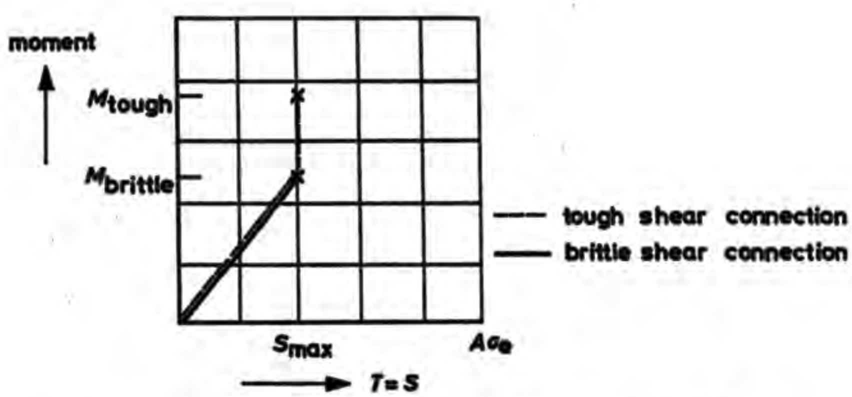

Relation between shear load and moment.

Fig.17

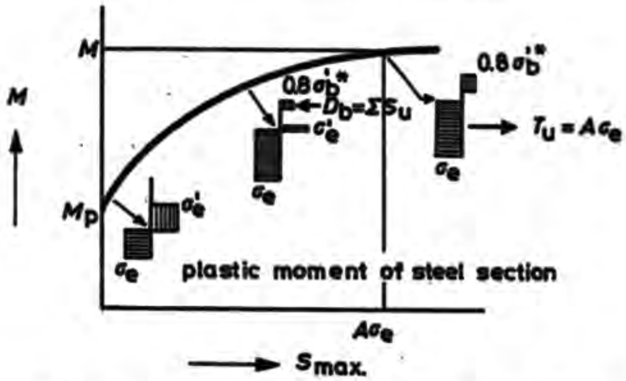

Relation between M and $S_{max.}$ for a tough shear connection.

Fig.18

test no.	loading scheme	measured moment and shear force at failure			failure mode
		M_{max} (kNm)	[illegible]	$V_{max.}$ (kN)	
3	4,00	16,7	0,69	16,7	shear failure
4	2,00 2,00 / 4,00	16,7	0,77	10,7	" "
5	3,00 / 4,00	13,7	0,56	24,7	" "
6	0,50 3,00 0,50 / 4,00	12,2	0,50	21,7	" "
7	3,00 / 4,00 2 x 6 shear connectors	24,3	1,0	56,7	flexural failure

Results of tests on Holorib - slabs.

Fig.19

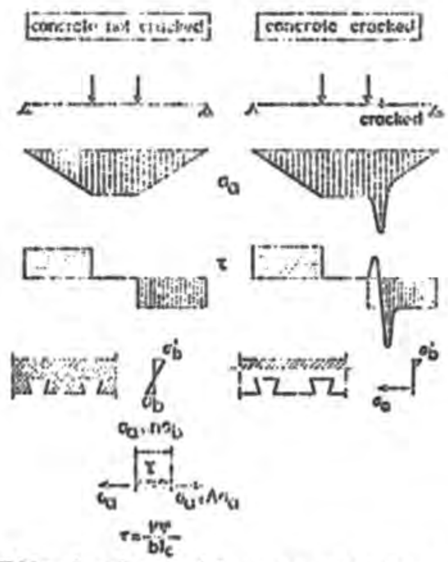

Fig.20 Effect of cracking on the horizontal shear forces in a Holorib-type composite slab.

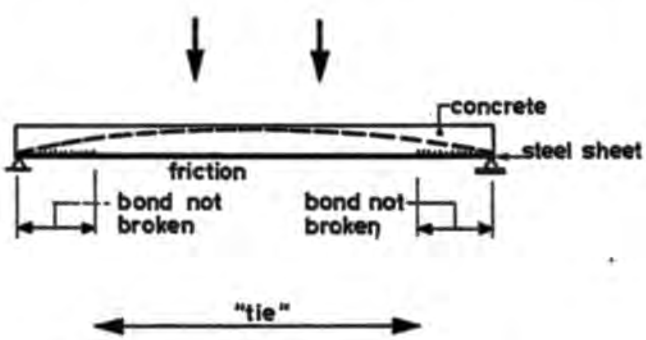

Illustration of composite action in a Holorib-type composite floor after bond is partly destroyed.

Fig.21

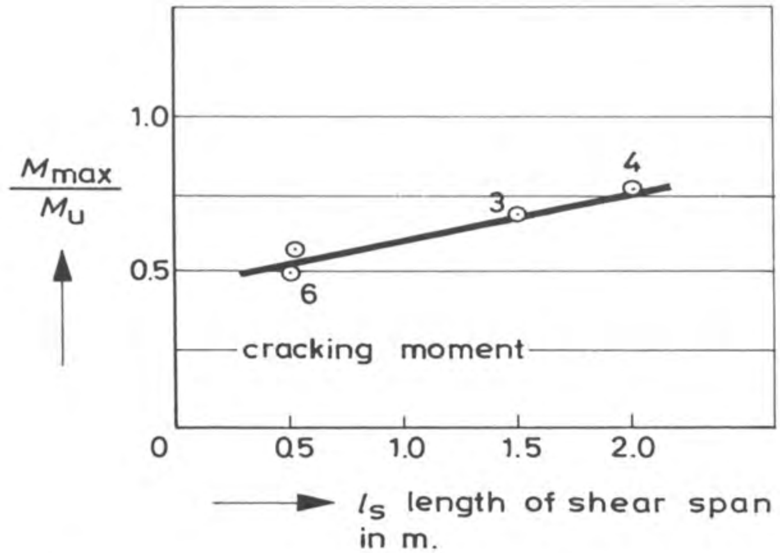

Ultimate moment as a function of the lenght of the shear span.

Fig. 22

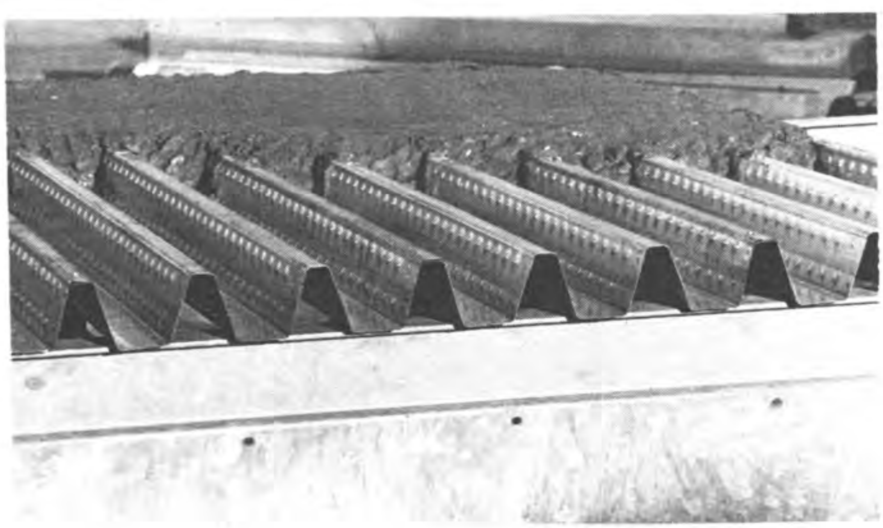

Composite floor system "Prins"

Fig. 23

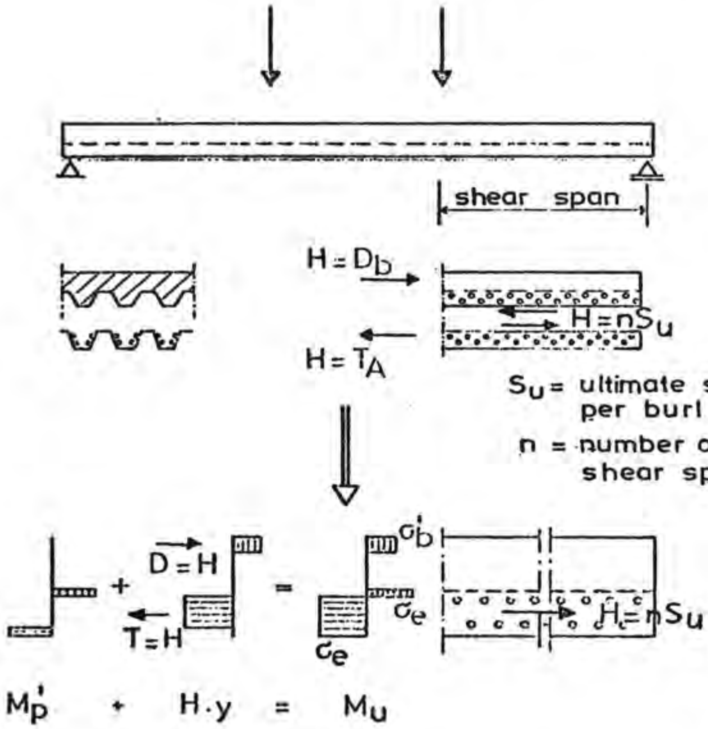

Stress distribution at ultimate load.

Fig. 24

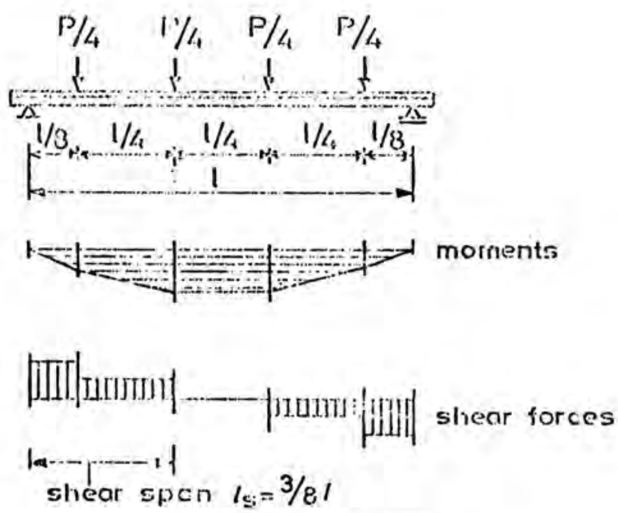

Test scheme

Fig.25

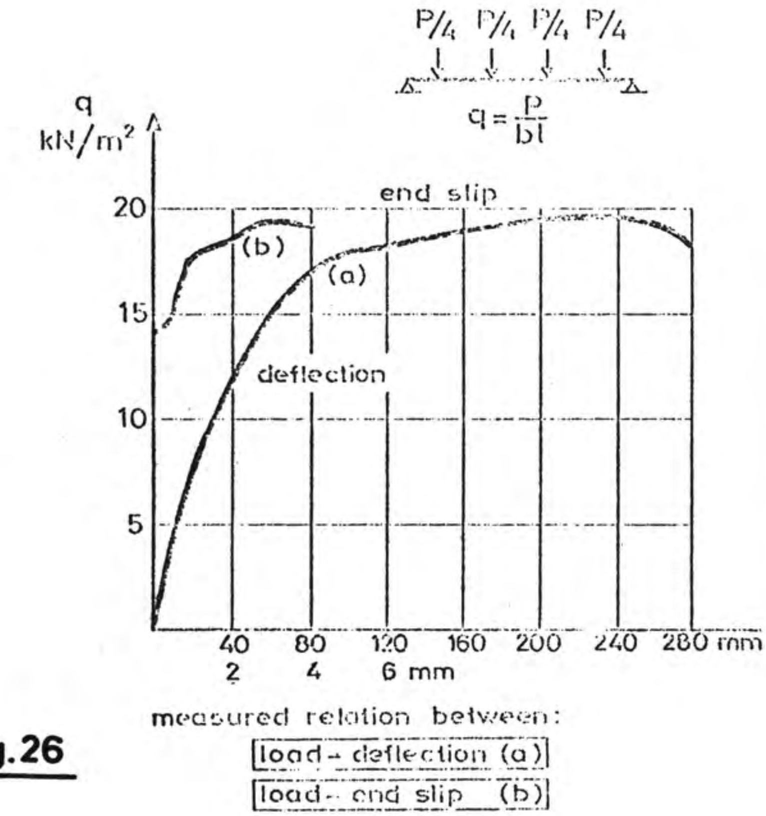

Fig. 26

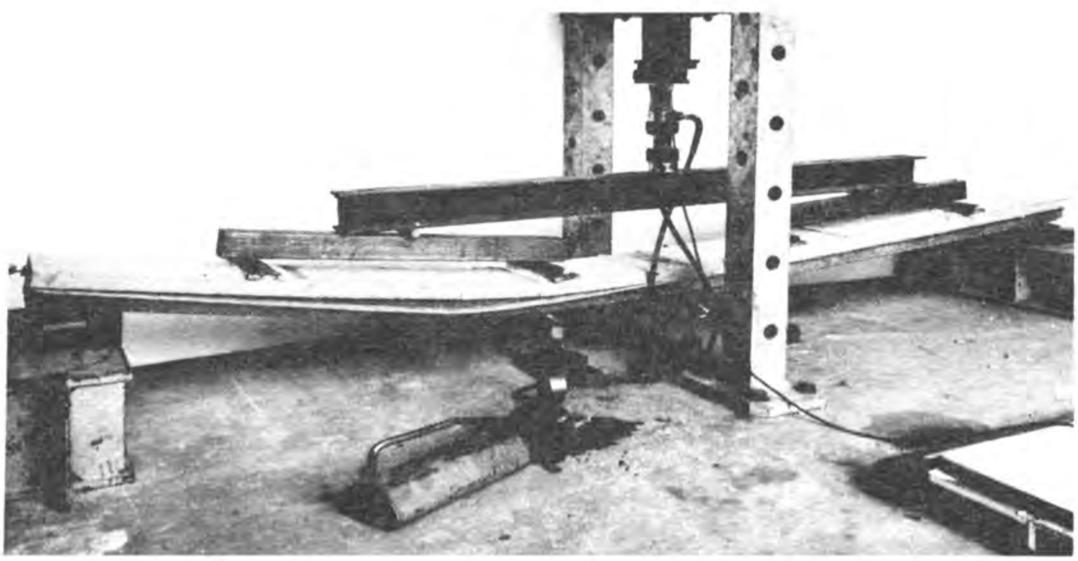

Fig. 27 Test specimen after failure

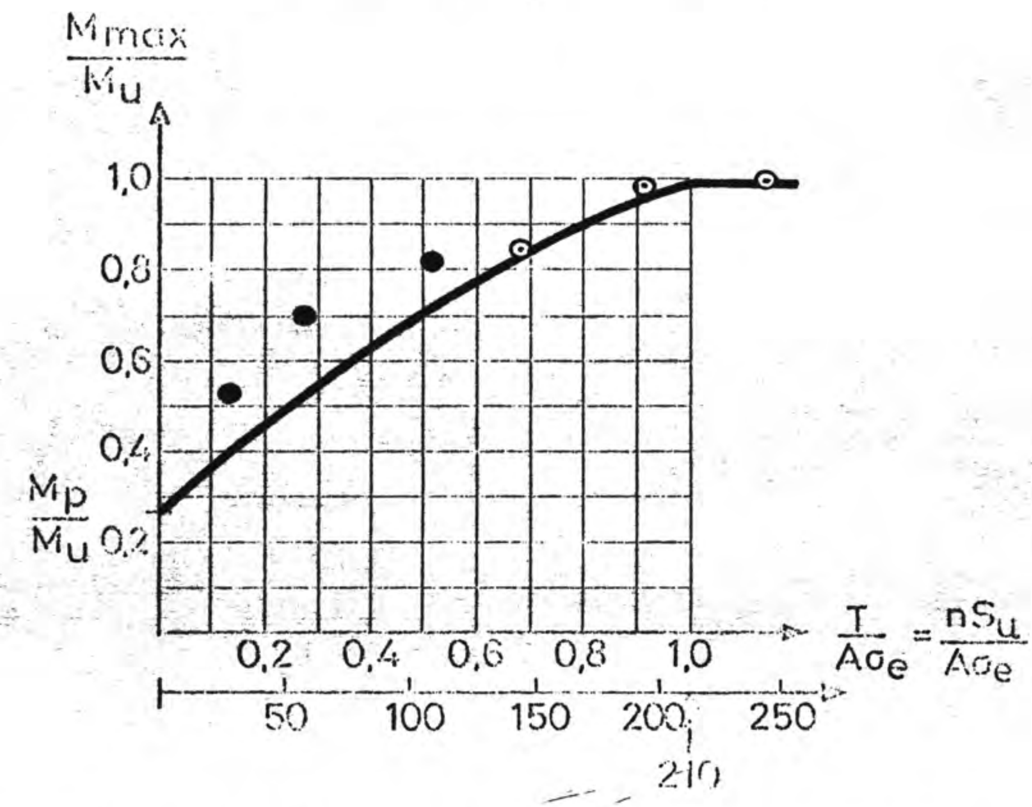

Fig. 28 Relation between maximum moment and the number of burls in the shear span.

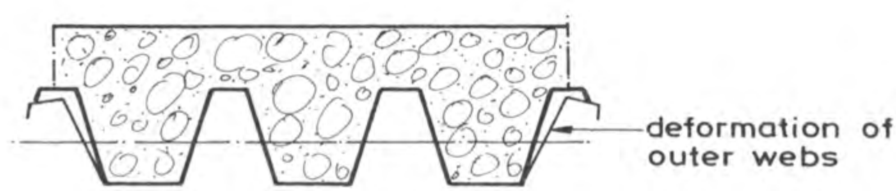

In the tests the lateral unsupported webs deformed.

Fig.29

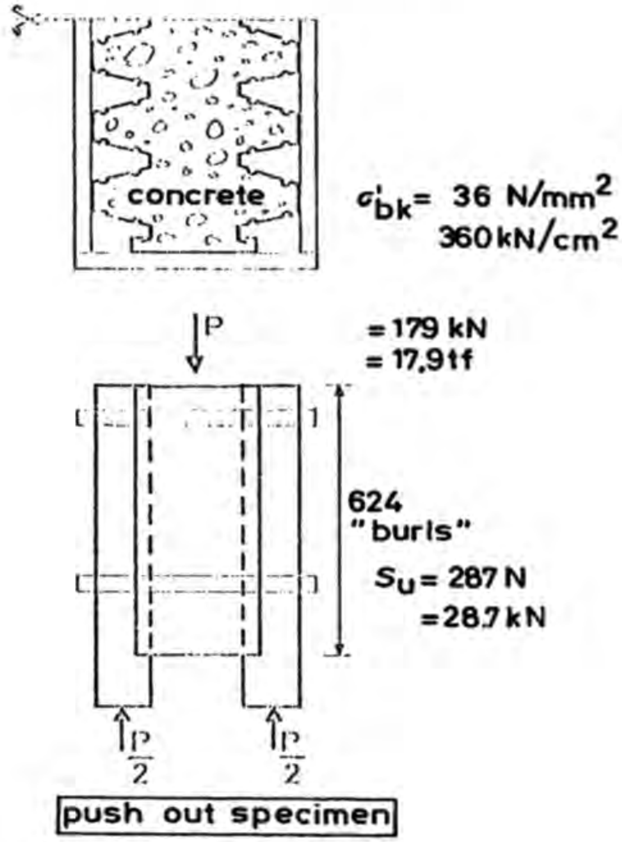

Push out specimen as used for the tests on "Prins-floor."

Fig. 30